Further evidence for a spin-glass phase transition in amorphous Fe-Mn-P-B-Al alloys

R. B. Goldfarb

National Bureau of Standards, Boulder, Colorado 80303

K. V. Rao

Central Research Laboratories, 3M Center, St. Paul, Minnesota 55133

H. S. Chen

Bell Laboratories, Murray Hill, New Jersey 07974

C. E. Patton

Colorado State University, Fort Collins, Colorado 80523

Low field dc susceptibility, thermoremanent magnetization, and hysteresis studies are presented for two amorphous Fe-Mn-P-B-Al alloys of concentrations close to, and on either side of, the multicritical point in the magnetic phase diagram. They exhibit spin-glass and para-ferro-spin-glass transitions, respectively. For the spin-glass alloy, the Edwards–Anderson-type order parameter deduced from the dc susceptibility is found to yield a mean-field-valued critical exponent. In the alloy with two magnetic transitions, the temperature dependence of the thermoremanence and hysteresis indicate a ferro-spin-glass transition temperature consistent with that deduced from a scaling approach for the same alloy system.

PACS numbers: 75.50.Kj, 75.30.Kz, 75.40. – s

INTRODUCTION

The nature of transitions to the ordered state in systems with random, competing exchange interactions continues to be an interesting and challenging aspect of the problem of disordered systems. Some models proposed to explain such random systems predict a multicritical point, MCP, in the magnetic phase diagram at which the ferromagnetic transition line intersects the line of spin-glass transitions whenever the mean of the distribution of exchange energies, $\mathcal{J}_o$, becomes comparable to its width, $\mathcal{J}$ [1–3]. The magnetic phase diagrams of such random-bond, quenched, bulk magnetic systems predict transitions from paramagnetic to spin-glass as well as paramagnetic to ferromagnetic to spin-glass as a function of decreasing temperature. The latter is expected to occur for alloy concentrations corresponding to values of $\mathcal{J}_o/\mathcal{J}$ lying between 1 and 1.2. Experimental realization of such phase diagrams has been reported for a number of Fe and Co based amorphous alloys of the type $(Fe/Co_{1-x}T_x)_{75}P_{16}B_6Al_3$, where T = Ni, Mn, Cr, etc. [4], as well as crystalline Fe-Al [5], Pd-Fe-Mn [6], Fe-Cr [7], Eu-Sr-S [8], and Au-Fe [9] alloys. The first detailed, quantitative critical-point studies of such a phase diagram close to the MCP were for amorphous Fe-Mn-P-B-Al and Fe-Ni-P-B-Al alloys [10–12] showing that the spin-glass and the ferromagnetic lines satisfy a scaling hypothesis appropriate to the MCP common to these lines, and also that the ferromagnetic–spin-glass transition is of a continuous second-order type. The results of recent small-angle neutron-scattering experiments [13] on $(Fe_{1-x}Mn_x)_{80}P_{16}C_4$ support the above point of view. In particular these experiments demonstrate the existence of a sharp, well-defined peak at the spin freezing temperature T_f, below the Curie temperature T_C, which approaches the one at T_C and collapses into a single peak for alloy concentrations close to the MCP. Nevertheless, details of the nature of the transitions mentioned above, and especially the behavior of these systems at temperatures below these transitions, are far from clear. In particular the existence of a double transition (para–ferro–spin-glass) for decreasing temperature has been actively pursued theoretically. It has even been suggested that there exist a number of transitions due to the possible coexistence of ferromagnetic and spin-glass order [14,15]. In the present paper, detailed low-field dc susceptibility χ_{dc}, thermoremanent magnetization TRM, and dc hysteresis loop studies are presented for two concentrations lying close to, and on either side of, the MCP in the amorphous Fe-Mn-P-B-Al alloy system. For the spin-glass alloy, the Edwards–Anderson-type order parameter [16] deduced from χ_{dc} below T_f is found to yield a mean-field-valued critical exponent [1]. The magnetic-field dependence of the magnetization and the TRM data for the alloy with two magnetic transitions indicate a ferro–spin-glass transition temperature consistent with that reported based on a scaling approach for the same alloy system [10].

EXPERIMENT

The amorphous ribbon samples used in this work, prepared by a melt-spinning technique [17], were obtained from the same stock as those used in recent neutron diffraction studies [18]. Atomic absorption and microprobe analysis were in agreement on the Fe and Mn concentrations. The alloys used in this study were $(Fe_{0.648}Mn_{0.352})_{75}P_{16}B_6Al_3$ & $(Fe_{0.676}Mn_{0.324})_{75}P_{16}B_6Al_3$, hereafter referred to as alloys I and II respectively. Ten to 15 ribbon segments about 1 cm long, 1 mm wide, and roughly 0.1 mm thick were stacked together for dc magnetization studies. Measurements were made along the axis of the sample width in the plane of the ribbons using a vibrating-sample magnetometer in the temperature range 4–300 K, and in applied magnetic fields ranging from 4×10^3 A/m (50 Oe) to 6.4×10^5 A/m (8 kOe). Temperature was measured using a GaAs diode calibrated to ±0.5 K. The demagnetization factor for the configuration of the sample was estimated to be very small, about 0.03–0.07 SI (0.38–0.84 cgs). Consequently, the internal and external fields and susceptibilities are about equal.

Contribution of the National Bureau of Standards, not subject to copyright.

 0021-8979/82/032217-03$02.40 © 1982 American Institute of Physics

Downloaded 09 May 2003 to 129.82.31.230. Redistribution subject to AIP license or copyright, see http://ojps.aip.org/japo/japcr.jsp

RESULTS AND DISCUSSION

Spin-glass alloy I: $(Fe_{0.648}Mn_{0.352})_{75}P_{16}B_6Al_3$

It has been shown that the line of the ac susceptibility peaks in this amorphous system obeys scaling laws and can therefore be looked upon as a critical line [12]. In the present work, the details of a typical spin-glass transition across that line are presented. Figure 1 shows the susceptibility (mass magnetization σ divided by applied field H) for the zero-field cooled (ZFC) alloy in different measuring fields. Also shown are the field cooled (FC) and thermoremanent magnetization (TRM) curves for a field of 8×10^3 A/m (100 Oe). The ZFC plus TRM curves add to approximately the FC curve, as expected. Both the ZFC and FC curves indicate a finite susceptibility as temperature approaches zero. The TRM flattens out above T_f. In this figure the absolute value of susceptibility has an uncertainty of $\pm1.3\times10^{-5}$ m^3/kg ($\pm10^{-3}$ cm^3/g).

From the peak in the FC curve, T_f is 40 K. The

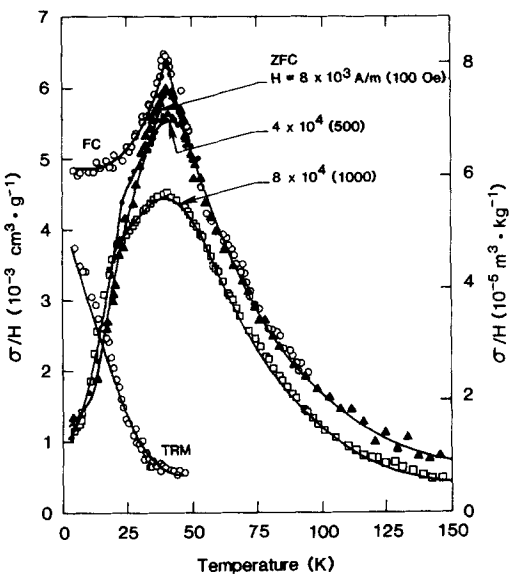

Fig. 1. Susceptibility (magnetization σ divided by applied field H) versus temperature upon warming alloy I. FC, ZFC, and TRM denote the field cooled, zero-field cooled, and thermoremanence curves, respectively.

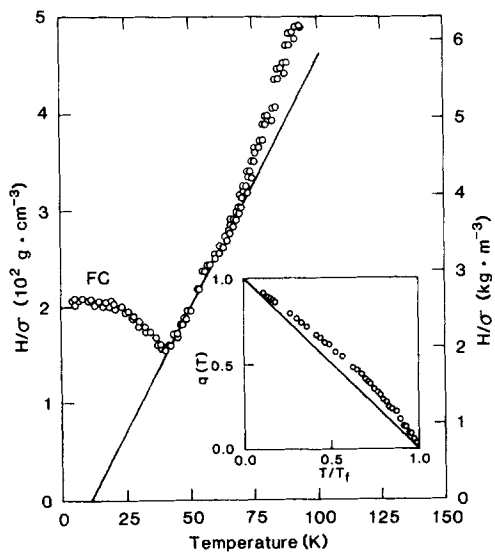

Fig. 2. Inverse susceptibility versus temperature for the FC curve shown in Fig. 1. The data yield the spin-glass order parameter q(T) shown in the inset.

cusp is unusually sharp considering the magnitude of the measuring field and the proximity of the composition to the MCP. Such sharpness is typical in rapidly quenched spin glasses which are inevitably free from many metallurgical problems commonly encountered in crystalline systems. While the susceptibility peak is rounded as expected for higher H, T_f is nearly independent of H. This suggests a collective freezing of the spins at T_f.

The FC curve was examined in detail, as it corresponds to the state of thermodynamic equilibrium. The ratio, $\chi(0)/\chi(T_f)$ for the FC curve is found to be 0.75. Sherrington and Southern [19] related this ratio to the local spins via the equation

$$\chi(0)/\chi(T_f) = (2/3\pi)^{1/2}\,[(2S+1)^2+1]^{1/2}/(S+1). \qquad (1)$$

This relation restricts the value of the susceptibility ratio to between 0.69 (spin ½) and 0.92 (spin ∞), consistent with the present value of 0.75. The inverse susceptibility versus temperature is shown in Fig. 2. A Curie-Weiss law is followed above T_f, yielding a Curie constant C of 0.19 K·cm^3/g and a Weiss constant Θ of 11 K. The value of C implies an average value of 10 μ_B per transition-metal atom. The spin-glass order parameter q(T), calculated using the relation [1,20,21]

$$q(T) = 1 - T\,\chi(T)/[C+\Theta\,\chi(T)], \qquad (2)$$

is shown in the inset in Fig. 2 for temperatures below T_f. The temperature axis is normalized and the solid line shows the Sherrington–Kirkpatrick mean-field prediction [1]. The agreement is reasonable, implying a critical exponent β of approximately 1.

Para–ferro–spin-glass alloy II:
$(Fe_{0.676}Mn_{0.324})_{75}P_{16}B_6Al_3$

The magnetization of alloy II for a range of fields 4×10^3 A/m (50 Oe) to 6.4×10^5 A/m (8 kOe) is shown in Fig. 3. Qualitatively, both the applied-field and temperature dependence of the magnetization observed here is rather similar to that for an Fe-Mn alloy of composition $(Fe_{0.68}Mn_{0.32})_{75}P_{16}B_6Al_3$ reported by Yeshurun et al. [11]. For that alloy, on the basis of a scaling analysis technique, a Curie temperature T_C of 100 K followed by a ferro–spin-glass-type transition at a temperature T_{fg} of 38 K were reported. From the details of the magnetic phase diagram given in Ref. 11, it is clear that in this regime the separation between the two transition temperatures varies strongly with Mn

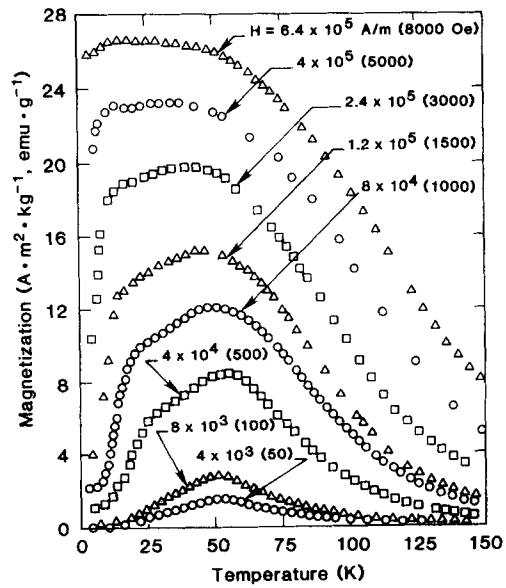

Fig. 3. Magnetization σ upon warming alloy II after zero-field cooling for different measuring fields. Measuring fields H are given in A/m (SI) and Oe (cgs).

Downloaded 09 May 2003 to 129.82.31.230. Redistribution subject to AIP license or copyright, see http://ojps.aip.org/japo/japcr.jsp

concentration. Thus for the alloy studied here it is expected that T_C and T_{fg} would be closer together, though the increase in Mn concentration is rather small. Based on the accurate determination of the alloy compositions in Ref. 4 and the present work, it is believed that alloy II is slightly to the ferromagnetic side of the MCP on the magnetic phase diagram, though it is by no means a soft ferromagnet (susceptibility is not limited by the reciprocal of the demagnetization factor).

Figure 4 shows the susceptibility (mass magnetization σ divided by measuring field H) for the ZFC and FC cases and the TRM for a field of 4×10^3 A/m (50 Oe). The semilog plot highlights the low-temperature data. Below 12 K, the TRM and FC curves are flat, suggestive of substantially complete spin freezing with respect to the 4×10^3 A/m (50 Oe) measuring field. There is a change in the temperature rate of decay of the TRM at 40 K. The FC and ZFC curves also meet around 40 K. This

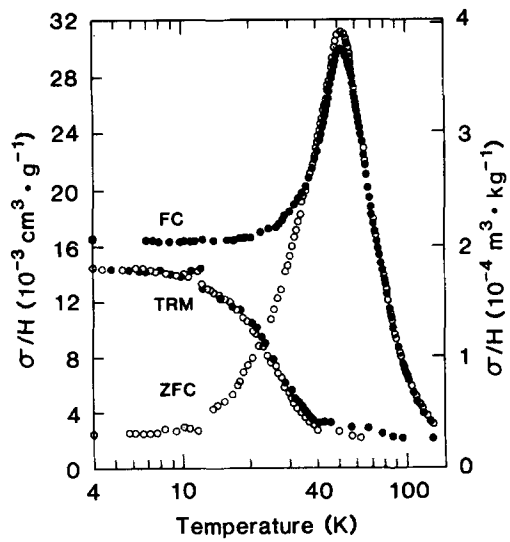

Fig. 4. Semilog plot of susceptibility versus temperature upon warming alloy II. FC, ZFC, and TRM denote the field cooled, zero-field cooled, and thermoremanence curves, respectively, for a field of 4×10^3 A/m (50 Oe). The TRM was measured twice.

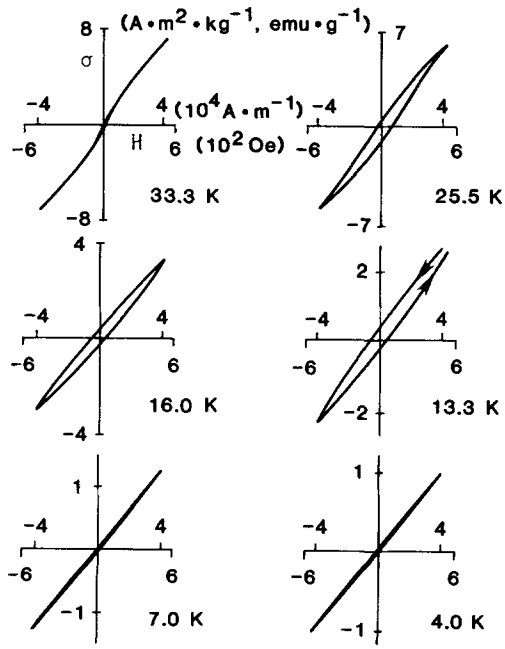

Fig. 5. Hysteresis loops at six representative temperatures obtained after zero-field cooling alloy II. Note that the scales on the magnetization axis change.

temperature may be identified as T_{fg}. Note that the TRM persists above T_{fg}. The maximum in low-field magnetization does not correspond to any transition temperature but is an inevitable consequence of the long-range order giving in to a spin-glass-type behavior at low temperature [4].

Hysteresis loops were studied at temperatures below T_{fg}. For the maximum fields, $\pm4\times10^4$ A/m (±500 Oe), and times, ∿10 min, used to measure a loop, hysteresis is found to be negligible above 40 K. At ∿33 K, the loop opens. As seen from the temperature dependence of the shape of the loops in Fig. 5, maximum hysteresis with some time-dependent magnetic relaxation occurs near 26 K. At 16 K, there is relaxation and the hysteresis is somewhat reduced. At 13 K there is still considerable loss, but now the loop does not close upon itself, indicative of substantial relaxation. At 7 K the loop closes upon itself, relaxation is minimal, and losses are less, decreasing a bit further at 4 K. Note the changes in scale on the magnetization axis.

A maximum in the temperature dependence of the hysteresis loss as observed here is often seen in mictomagnetic/spin-glass alloys [22,23]. The temperature of this maximum depends on the maximum applied field in such measurements. Therefore any unique determination of freezing temperatures from the temperature dependence of hysteresis loss or coercivity data could be misleading as, for example, in the case of low-field coercivity in amorphous Fe-Ni [24,25].

REFERENCES

[1] S. Kirkpatrick and D. Sherrington, Phys. Rev. B 17, 4384 (1978).
[2] M. W. Klein, L. J. Schowalter, and P. Shukla, Phys. Rev. B 19, 1492 (1979).
[3] J. H. Chen and T. C. Lubensky, Phys. Rev. B 16, 2106 (1977).
[4] Y. Yeshurun, M. B. Salamon, K. V. Rao, and H. S. Chen, Phys. Rev. B 24, 1536 (1981).
[5] R. D. Shull, H. Okamoto, and P. A. Beck, Solid State Comm. 20, 863 (1976).
[6] B. H. Verbeek, G. J. Nieuwenhuys, H. Stocker, and J. A. Mydosh, Phys. Rev. Lett. 40, 586 (1978).
[7] C. R. Fincher, S. M. Shapiro, A. H. Palumbo, and R. D. Parks, Phys. Rev. Lett. 45, 474 (1980).
[8] H. Maletta and P. Convert, Phys. Rev. Lett. 42, 108 (1979).
[9] B. R. Coles, B. V. B. Sarkissian, and R. H. Taylor, Phil. Mag. B 37, 489 (1978).
[10] M. B. Salamon, K. V. Rao, and Y. Yeshurun, J. Appl. Phys. 52, 1687 (1981), and references therein.
[11] Y. Yeshurun, M. B. Salamon, K. V. Rao, and H. S. Chen, Phys. Rev. Lett. 45, 1366 (1980).
[12] M. B. Salamon, K. V. Rao, and H. S. Chen, Phys. Rev. Lett. 44, 596 (1980).
[13] B. D. Rainford, S. K. Burke, J. R. Davis, and W. Howarth (to be published).
[14] M. Gabay and G. Toulouse, Phys. Rev. Lett. 47, 201 (1981).
[15] A. J. Bray and M. A. Moore, J. Phys. C: Solid St. Phys. 13, 419 (1980).
[16] S. F. Edwards and P. W. Anderson, J. Phys. F: Metal Phys. 5, 965 (1975).
[17] H. S. Chen and C. E. Miller, Mat. Res. Bull. 11, 49 (1976).
[18] G. Aeppli, S. M. Shapiro, R. J. Birjeneau, and H. S. Chen (to be published).
[19] D. Sherrington and B. W. Southern, J. Phys. F: Metal Phys. 5, L49 (1975).
[20] T. Mizoguchi, T. R. McGuire, S. Kirkpatrick, and R. J. Gambino, Phys. Rev. Lett. 38, 89 (1977).
[21] S. Nagata, P. H. Keesom, and H. R. Harrison, Phys. Rev. B 19, 1633 (1979).
[22] J. S. Kouvel, J. Phys. Chem. Solids 21, 57 (1961).
[23] R. B. Goldfarb and C. E. Patton, Phys. Rev. B 24, 1360 (1981), Figs. 5 and 10.
[24] S. M. Bhagat, J. A. Geohegan, and H. S. Chen, Solid State Comm. 36, 1 (1980).
[25] J. A. Geohegan and S. M. Bhagat (to be published).

Downloaded 09 May 2003 to 129.82.31.230. Redistribution subject to AIP license or copyright, see http://ojps.aip.org/japo/japcr.jsp